Liquid Crystals
Publication details, including instructions for authors and subscription information:
http://www.informaworld.com/smpp/title~content=t713926090

Thermotropic liquid crystalline comb-like polymers with polyacrylamide main chain. (2) Influence of the nature of the substituents of the biphenyl mesogenic core

Bernard Gallot[a]; Florence Monnet[a]; Siyuan He[a]
[a] Laboratoire des Matériaux Organiques à Propriétés Spécifiques, Vernaison, France

To cite this Article Gallot, Bernard , Monnet, Florence and He, Siyuan(1995) 'Thermotropic liquid crystalline comb-like polymers with polyacrylamide main chain. (2) Influence of the nature of the substituents of the biphenyl mesogenic core', Liquid Crystals, 19: 4, 501 — 509

To link to this Article: DOI: 10.1080/02678299508032012

URL: http://dx.doi.org/10.1080/02678299508032012

LIQUID CRYSTALS, 1995, VOL. 19, NO. 4, 501–509

Thermotropic liquid crystalline comb-like polymers with polyacrylamide main chain. (2) Influence of the nature of the substituents of the biphenyl mesogenic core†

by BERNARD GALLOT*, FLORENCE MONNET and SIYUAN HE
Laboratoire des Matériaux Organiques à Propriétés Spécifiques, CNRS,
BP 24, 69390 Vernaison, France

(*Received 6 April 1995; accepted 24 May 1995*)

Comb-like polymers with polyacrylamide main chains and three types of lipophilic biphenyl side chains have been synthesized and their thermotropic behaviour has been determined. All the polymers exhibit two smectic mesophases as a function of temperature, but the nature of the smectic mesophases is governed by the nature of the substituent *R* of the biphenyl core. For R = H, the polymers exhibit a double layer, ordered, tilted smectic S_{I_2} and a double layer, disordered, tilted smectic S_{C_2}. For R = CN, the polymers exhibit a double layer, disordered, tilted smectic S_{C_2} and a double layer, disordered, perpendicular smectic S_{A_2}. For $R = O\text{–}CH_2\text{–}CH(CH_3)\text{–}C_2H_5$, the polymers exhibit a double layer, ordered, tilted smectic S_{F2} and a double layer, disordered, tilted smectic S_{C_2}, these two structures being chiral when the substituent *R* is chiral. Comparison of the thermotropic behaviour of the polyacrylamide polymers with that of polymers with the same mesogenic cores but different main chains shows the high smectogenic power of the polyacrylamide skeleton.

1. Introduction

Recently we showed that comb-like polymers with a polyacrylamide main chain and undecanoylbiphenyl side chains exhibit, as a function of temperature, a tilted, ordered, bilayer smectic phase S_{I_2} and a tilted, disordered, bilayer smectic phase S_{C_2} [1] and thus confirmed the high smectogenic tendency of polyacrylamide polymers already observed for polymers with lipopeptidic [2–4] or liposaccharidic [5] side chains. In order to improve the electro-optic properties of the polyacrylamide smectic polymers, we undertook the synthesis of comb-like polymers with biphenyl mesogenic side chains bearing either a chiral *S*(-)-2-methyl-1-butoxy group to induce chiral smectic phases able to exhibit ferroelectric properties or a highly polar carbonitrile group to induce NLO activity. We also synthesized polymers with a non-chiral, racemic 2-methyl-1-butoxy group to determine if the chirality of the biphenyl substituent has an influence on the smectic phases.

In the present paper, we will describe the synthesis and the thermotropic behaviour of comb-like polymers with a polyacrylamide main chain, spacers, containing ten methylene groups and biphenyl-based mesogenic units, and discuss the influence of the substituent *R* of the biphenyl core. Our comb-like polymers correspond to the formula:

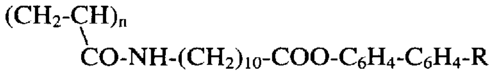

$$\begin{array}{l}(CH_2\text{-}CH)_n \\ \qquad \backslash \\ \qquad CO\text{-}NH\text{-}(CH_2)_{10}\text{-}COO\text{-}C_6H_4\text{-}C_6H_4\text{-}R\end{array}$$

with R = H, CN, $O\text{-}CH_2\text{-}CH(CH_3)\text{-}C_2H_5$.

2. Experimental

2.1. *Materials*

Dicyclohexylcarbodiimide (DCC), 4-pyrrolidinopyridine (PPY), 11-aminoundecanoic acid (**I**), 4-toluenesulphonyl chloride, 2-methylbutan-1-ol, 4-hydroxybiphenyl and 4′-hydroxybiphenyl-4-carbonitrile from Aldrich and *S*(-)-2-methylbutan-1-ol from Fluka were used as received. The chiral and non-chiral 4-hydroxy-4′-(2-methylbutyloxy)biphenyls were prepared from 2-methylbutan-1-ol and *S*(-)-2-methylbutan-1-ol as described in the literature [6, 7]. Acryloyl chloride from Aldrich was distilled under vacuum. α, α,′-azobis-isobutyronitrile (AIBN, 99 per cent purum from Merck) was recrystallized before use. Solvents were purified by classical methods.

---

* Author for correspondence.

† Presented in part at the International Conference on Liquid Crystal Polymers, 6–9 September, 1994, Beijing, China.

0267–8292/95 $10·00 © 1995 Taylor & Francis Ltd.

2.2. *Synthesis of the monomers* (**IIIa–c**)

11-Acryloylamidoundecanoic acid (**II**) was synthesized as already described [1, 5] in a yield of 95 per cent and with a melting point of 84°C.

Monomer (**IIIa**): *R* = *H* was synthesized as already described [1] in a yield of 56 per cent and with a melting point of 115°C.

Monomer (**IIIb**): *R* = *CN*. A solution of 5·1 g (20 mmol) of 11-acryloylamidoundecanoic acid (**II**) in 100 ml of dry CH_2Cl_2 was degassed under an inert atmosphere. Then 4·02 g (20 mmol) of 4′-hydroxybiphenyl-4-carbonitrile and 3·02 g (20 mmol) of PPY were added. The solution was cooled to 0°C and a solution of 4·16 g (20 mmol) of DDC in 20 ml of CH_2Cl_2 added dropwise. After 20 min at 0°C and 68 h at room temperature, the solution was filtered to remove the precipitate of DCU; the filtrate was washed first with 0·5 M HCl and then with saturated aqueous $NaHCO_3$; the organic solution was dried over $MgSO_4$ and evaporated. The precipitate was recrystallized from acetonitrile at 64°C. The precipitate obtained by cooling was filtered off, washed with acetonitrile and dried under vacuum (yield 83 per cent). TLC: R_f = 0·37; eluant: $AcOEt/C_6H_{12}/CHCl_3$ (3/3/5). FTIR (Nicolet 20SX), cm^{-1}: 32955, 1653, 1542 (amide), 2921, 2851 (aliphatic chain), 1748 (ester), 1625 (vinyl), 2227 ($C{\equiv}N$). ^1H NMR, 250 MHz, ($CDCl_3$, TMS) ppm: 7·8–7·1 (H aromatic), 6·0–6·3 (H_b and H_c), 5·6 (H_a, 5·85 (–NH–), 3·3 (t, H_1), 2·58 (t, H_{10}), 1·78 (m, H_2), 1·55 (m, H_9), 1·3 ($H_3 = NH_8$).

Monomer (**IIIc**): *R* = $O{-}CH_2{-}CH(CH_3){-}C_2H_5$ was prepared in the same way as (**IIIb**) in a yield of 77 per cent from 5·1 g (20 mmol) of **II** and 5·12 g (20 mmol) of 4-hydroxy-4′-(2-methylbutyloxy)biphenyl. FTIR, cm^{-1}: 3301, 1655, 1542 (amide), 2920, 2850 (aliphatic chain), 1745 (ester), 1624 (vinyl).

^1H NMR, 250 MHz, ($CDCl_3$, TMS) ppm: 7·6–6·9 (H aromatic), 6·3–5·9 (H_b and H_c), 5·6 (H_a), 5·65 (–NH–), 3·8 (m, H_{11})3·3 (t, H_1). 2·58 (t, H_{10}), 1·75 (m, H_2), 1·55 (m, H_9), 1·35 (H_3–H_8), 1·05 (d, H_{15}), 0·95 (t, H_{14}).

2.3. *Polymerization*

Polymers IVa1 and IVa2 were obtained by radical polymerization in THF solution as already described [1].

Polymers IVb1 and IVb2 were obtained by polymerization of the monomer IIIb (2·0 g) in chloroform solution (50 ml), under vacuum, for 80 h, at 73°C, using AIBN (0·034 mg) as initiator.

Chiral polymer IVc1 was obtained by polymerization of the chiral monomer IIIc (2·0 g) in THF solution (20 ml), under vacuum, for 4 d, at 68°C, using AIBN (0·031 mg) as initiator.

Non-chiral polymer IVc2 was obtained under similar conditions using the non-chiral monomer IIIc.

Non-chiral polymer IVc3 was prepared as follows: 2 g of monomer **III** were solubilized in 20 ml of THF and degassed under argon; then 0·04 g of AIBN was added. The solution was maintained at 68°C for 80 h under argon and with agitation. Several samples were taken at various reaction times, and injected into GPC columns. The degree of conversion was determined from the ratio of the areas of the polymer and monomer + polymer peaks.

The polymers were recovered by precipitation once or twice in methanol.

2.4. *Characterization of the polymers*

Polymers were characterized by ^1H NMR at 250 MHz using $CDCl_3$ solutions and an AC 250 Brucker apparatus.

The molecular characteristics of the polymers (M_n, M_W and M_W/M_n) in THF or $CHCl_3$ were determined by light scattering (Brookhaven), and by Gel Permeation Chromatography (PSS gel mixed b columns, Waters 510 pump, Waters R410 refractometer, Software GPChrom LMOPS) using polystyrene calibration and THF or $CHCl_3$ as eluent.

2.5. *Polarization microscopy*

Optical polarization microscopic observations of the mesophase textures were carried out on thin films between glass slides without any previous treatment, using a Leitz Laborlux 12 POL microscope equipped with a Mettler heating stage FP 82 and control system FP 80.

2.6. *X-ray diffraction*

X-ray diffraction experiments were performed on unoriented samples with a Guinier-type focusing camera operating under vacuum, equipped with a bent quartz monochromator (reflection 101) giving a linear collimation of strictly monochromatic X-rays (CuK_{α_1}, λ = 1·54 Å) and a device for recording the diffraction patterns from samples at various temperatures between 20 and 200°C while controlling the temperature within less than 1°C. Several exposures were made in order to measure the strongest and the weakest reflections. Experimental amplitudes of diffraction of the different orders of reflections from the smectic layers were corrected for the

Table 1. Amplitudes (after normalization to the amplitude of the third order reflection) of the low angle reflections of the different smectic phases.

Polymer	Mesophase	a_1	a_2	a_3
IVa1	S_{I_2}	0	0·2	1
	S_{C_2}	0	0·3	1
IVb1	S_{C_2}	0·3	0	1
	S_{A_2}	0·4	0	1
IVc1	S_{F_2}	0·5	0·2	1
	S_{C_2}	0·6	0·2	1

Lorentz polarization factor [8] and normalized so that the strongest reflection has an amplitude of one (see table 1).

In order to obtain a better resolution in the wide angle domain and to be able to study oriented samples, a home-made pin-hole camera, operating under vacuum, using Ni filtered Cu radiation was also used. This camera was equipped with an electric heating device operating between 20 and 300°C and controlling the temperature within less than 1°C, and specially designed to operate with capillaries containing powder or oriented samples.

Fibre patterns were recorded at room temperature, on fibres pulled out with tweezers from the liquid crystalline or isotropic melts at different temperatures.

3. Results

3.1. *Polymer synthesis*

Polymers were prepared from α,ω-aliphatic animo acids in 3 steps: fixation of the polymerizable group at the amino end, fixation of the mesogenic group at the carboxylic end, and radical polymerization of the monomer obtained (see figure 1).

In the first step, 11-aminoundecanoic acid **I** was transformed into the polymerizable acid **II**, by nucleophilic substitution between acryloyl chloride and its amino group in aqueous KOH solution.

In the second step, the polymerizable acid **II** was esterified by 4-hydroxybiphenyl in the presence of a coupling agent DCC and PPY which modifies the equilibrium of the reaction by formation of *N*-acylpyridinium salts that are more electrophilic and increase both the reaction speed and the reaction yield [9, 10].

The polymerizations of the monomers **III** were carried out with AIBN initiator using THF of chloroform solutions depending upon the solubilities of the monomers, at temperatures between 68°C and 73°C, generally under vacuum. Vacuum was replaced by an inert atmosphere of argon when determination of the polymerization kinetics was wanted. GPC in THF allowed quantification of the monomer consumption through the variation of the ratio of the areas of the polymer and monomer peaks as a function of time. In figure 2 is plotted the conversion versus time for the polymer IVc3 and one can see that, within the limits of accuracy of the GPC, a degree of conversion of 92 per cent was obtained in 70h.

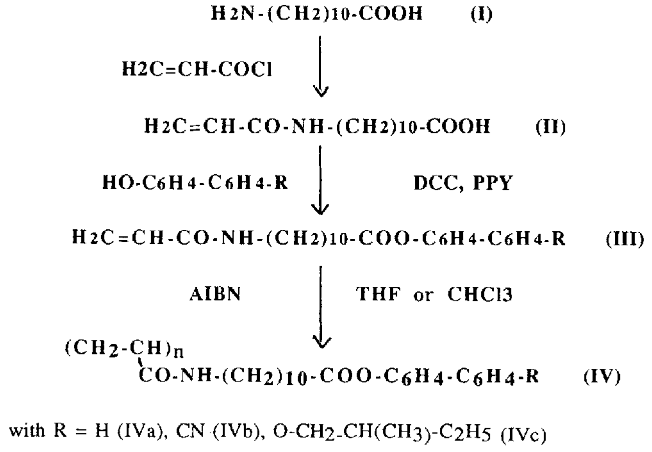

Figure 1. Scheme of synthesis of comb-like polyacrylamide polymers.

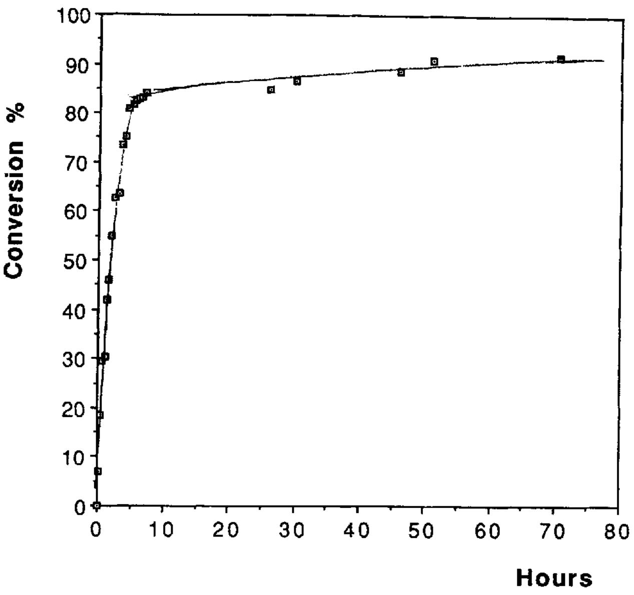

Figure 2. Conversion–time curve (from GPC) of the polymerization in THF solution of the 2-methyl-1-butoxy monomer.

Comparison of the molecular characteristics (see table 2) of the polymers shows that the molecular weights and the degrees of polymerization are quite high and the polydispersity index is rather low. Furthermore, molecular weights are higher when polymerization is carried out in chloroform rather than THF in agreement with the smaller transfer power of chloroform.

Table 2. Polymerization yields and molecular characteristics of the polymers studied. IVc1 is chiral while IVc2 and IVc3 are not chiral.

Polymer	Yield/per cent	M_n	M_w	M_w/M_n
IVa1	95	21600	38400	1·78
IVa2	95	24500	42300	1·73
IVb1	79	73100	94300	1·29
IVb2	76	68800	88100	1·28
IVc1	90	29000	42700	1·47
IVc2	85	14000	21500	1·54
IVc3	92	22200	27500	1·24

4. Liquid crystalline behaviour

4.1. *Description of the structures*

For the three types of polymers, all X-ray patterns recorded at temperatures between room temperature and isotropization temperature exhibit in the low angle domain two or three sharp reflections (see figure 3) and in the wide angle domain a sharp reflection (see figure 4) or a diffuse band (see figure 5) depending upon R and temperature.

The low angle reflections can be indexed as the 0 0 1 reflections of a lamellar structure. The wide angle reflection at 4·6 Å (see figure 4) is characteristic of a smectic structure with a hexagonal packing of the side chains (smectic B, F or I), [11]; the wide angle band at 4·6 Å (see figure 5) is characteristic of a disordered smectic structure (smectic A or C), [11].

In order to make a choice between the possible smectic structures, we have compared the thickness d of the smectic layers with the length L of the repeating unit of the polymers (corresponding to a monolayer structure) and the length $2l + p$ of 2 side chains and 1 main chain segment (corresponding to a bilayer structure) measured using CPK models with the spacer in an all *trans*-configuration (see table 3). One can see that d is much higher than L, but smaller than $2l + p$ for all polymers and phases except the upper phase of polymers IVb with a polar carbonitrile substituent, for which d is slightly higher than $2l + p$. So, for the upper phase of polymers IVb, the structure is of the double layer S_{A_2} type, while for the other mesophases the smectic structures are double layer smectic structures (F_2 or I_2 or C_2) with an angle to tilt ϕ given by $\cos \phi = d/(2l + p)$, or interdigitated, perpendicular smectic structures (B_d or A_d).

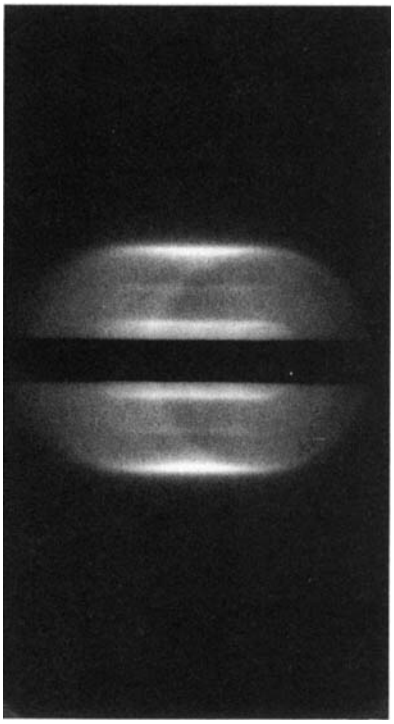

Figure 3. Focusing camera powder X-ray diagram of the S_{C_2} mesophase of the polymer IVc1 at 155°C.

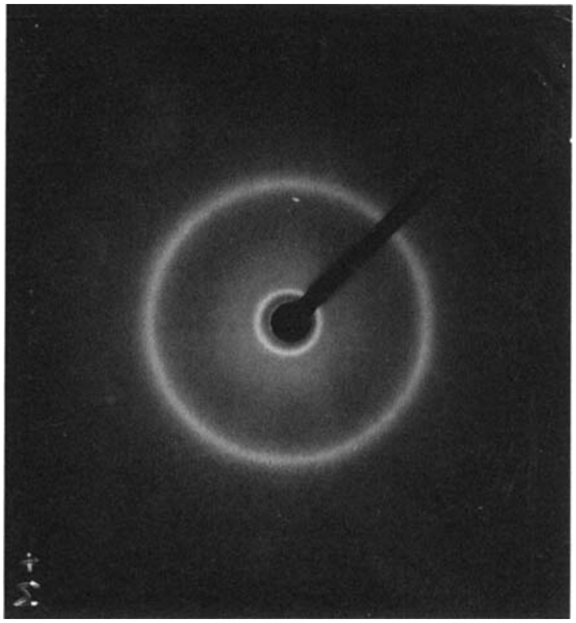

Figure 4. Pin-hole camera powder X-ray diagram of the S_{F_2} mesophase of the polymer IVc1 at 70°C, showing the third order small angle reflection and the wide angle sharp reflection; the first and second order small angle reflections are hidden by the beam-stop.

In order to distinguish tilted smectic structures from perpendicular smectic structures, we have used two methods: we have derived the intensity profiles $\rho(z)$ along the direction z perpendicular to the smectic planes from the intensities of the low angle reflections of the X-ray diagrams [8] on the one hand, and tried to draw oriented fibres of the polymers on the other hand. Unfortunately we succeeded in obtaining oriented fibres only in the case of the polymers IVb that have the highest molecular weights (see table 2).

Taking into account the fact that as many mesogenic cores are pointing in the $+z$ and $-z$ direction, and that we measure only the fluctuations around $\rho(\mathrm{o})$, the average electron density [8, 12], $\rho(z)$ is given by

$$\rho(z) = \Sigma a_n \cos(n 2\pi z/d).$$

Experimentally we measure the intensity of the diffraction orders so we lose the phase. Due to the symmetry of the electron density distribution, the phase factor and the structure factor must be 0 or π, so the a_n are real, but may be positive or negative. The phase problem then reduces to choosing the right combinations of sign for a_n ($n = 1$, 2, 3). For instance, $\rho + - + (z)$ will correspond to the

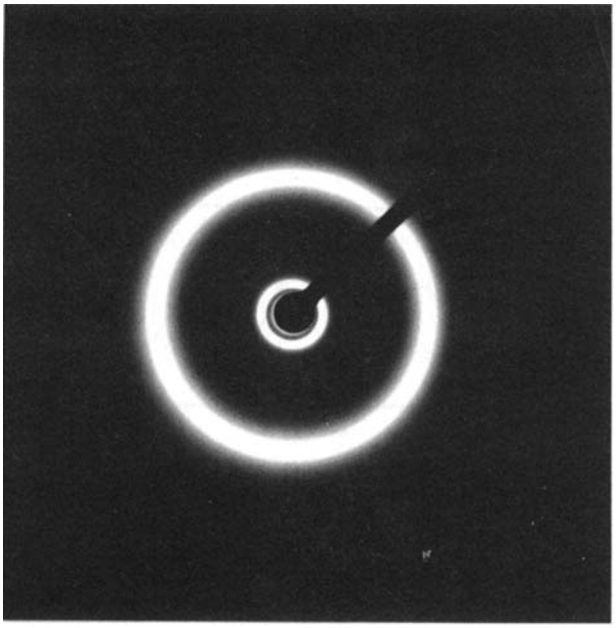

Figure 5. Pin-hole camera powder X-ray diagram of the S_{C_2} mesophase of the polymer IVc1 at 120°C, showing the third order small angle reflection and the wide angle diffuse band; the first and second order small angle reflections are hidden by the beam-stop.

Table 3. Type, structural parameters and domain of stability of the mesophases. $2l + p$ = length of 2 side chains and a main chain segment measured using molecular models; d = thickness of the smectic layers; ϕ = angle of tilt.

Polymer	$2l+p$/Å	d/Å	ϕ/°	Structure	Stability/°C
IVa	56·0	53·0	18·8	S_{I_2}	$T < 105$
	56·0	53·0	18·8	S_{C_2}	105–160
IVb	57·0	51·8	24·7	S_{C_2}	$T < 95$
	57·0	59·0	0·0	S_{A_2}	95–168
IVc	64·0	56·8	27·4	S_{F_2}	$T < 115$
	64·0	57·9	25·2	S_{C_2}	115–185

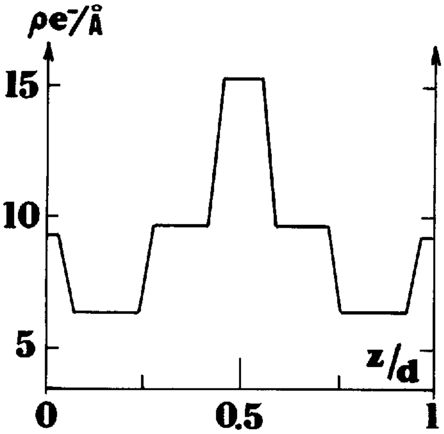

Figure 6. Schematic representation of the electron density profile of the partly interdigitated, perpendicular smectic structures S_{A_d} or S_{B_d}.

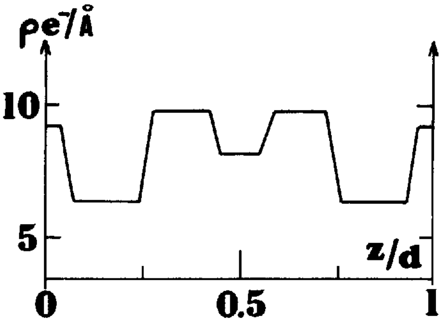

Figure 7. Schematic representation of the electron density profile of the tilted, bilayer smectic structures S_{C_2} or S_{F_2} or S_{I_2}.

combination where a_1 and a_3 are chosen positive while a_2 is chosen negative. As we observe 2 or 3 orders of diffraction, we obtain 4 or 8 combinations of sign for a_n—that is to say 4 or 8 electron density profiles $\rho(z)$.

In order to choose from the profiles the one that is physically acceptable, we calculated the electron densities of the different parts of the repeating unit of the polymer by dividing their numbers of electrons by their lengths measured using CPK models. We found: 9·2e⁻/Å for the skeleton, 6·4e⁻/Å for the paraffinic spacer and between 8·9 and 9·7e⁻/Å for the mesogenic groups, depending upon the nature of R.

In the case of an orthogonal interdigitated structure (S_{A_d} or S_{B_d}), one must observe a central maximum, corresponding to the partly interdigitated mesogenic groups, surrounded by 2 minima corresponding to the spacers and 2 secondary maxima corresponding to the polymeric skeleton (see figure 6).

In the case of a double layer tilted smectic structures S_{C_2} or S_{F_2} or S_{I_2}) one must observe a central minimum surrounded by 2 maxima corresponding to the mesogenic cores, 2 minima corresponding to the paraffinic spacers and 2 maxima corresponding to the polymeric skeleton (see figure 7).

We will examine successively the cases for the 3 types of polymers.

4.2. *Polymers (IVc)* $R = O\text{–}CH_2\text{–}CH(CH_3)\text{–}C_2H_5$

These polymers exhibit as a function of temperature an ordered smectic phase (sharp reflection in the wide angle domain) and a disordered phase (diffuse band in the wide angle domain), but for the 2 phases d is smaller than $2l + p$ (see table 3).

The 8 electron density profiles of the disordered smectic are represented in figure 8 (*a*)–(*h*). The 4 electron density profiles (*e*)–(*h*) are incompatible with both S_{A_d} and S_{C_2}

structures as they exhibit minima for the main chains and maxima for the paraffinic spacers. The 4 electron density profiles (*a*)–(*d*) are incompatible with a S_{A_d} structure as they exhibit minima in the middle of the layers where the mesogenic cores would be partially interdigitated; therefore the S_{A_d} structure must be rejected. On the contrary, they are in agreement with a S_{C_2} structure as they exhibit a minimum in the middle of the layer surrounded by maxima at the position of the mesogenic cores, minima at the position of the paraffinic spacers and maxima at the position of the polymeric skeleton. To choose from the 4 electron density profiles (*a*)–(*d*) the one that is most probable, we have to compare the electron densities of the mesogenic cores and the main chain on the one hand, and of the 2-methyl-1-butoxy tails and methylene spacers on the other hand. The electron density is higher for the biphenyl mesogenic core (9·7) than for the main chain (9·2), and higher for the tail (8·1) than for the spacer (6·4). Therefore, the best electron density profile is profile (*c*) corresponding to $\rho(z)$- + + .

The structure factors of the ordered smectic phase are very similar to those of the disordered phase (see table 1), and therefore the electron density profiles are also very similar. Consequently they are incompatible with an interdigitated smectic (S_{B_d}), but four of them are in agreement with a double layer, tilted smectic S_{F_2} or S_{I_2}, and we have only represented in figure 9 the electron density profile $\rho(z)$- + + that corresponds to the best agreement with the relative electron densities of the different parts of the repeating unit of the polymer.

Therefore we can conclude that the upper mesophase is a double layer, tilted and disordered S_{C_2} phase, while the lower mesophase is a double layer, tilted and observed S_{F_2} or S_{I_2} phase. It is difficult to distinguish the S_F phase from the S_I phase. Nevertheless, the single outer reflection of the

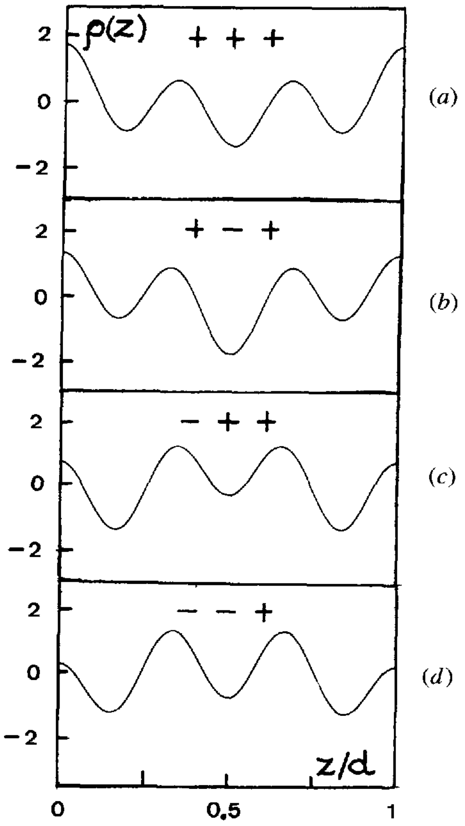

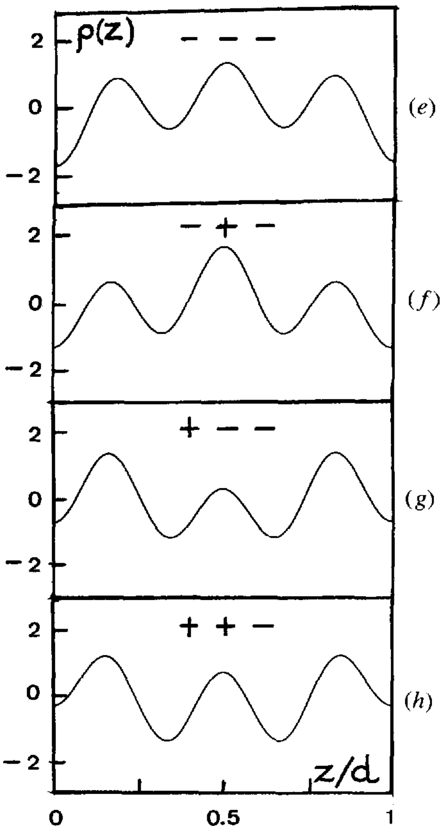

Figure 8. Projections of the electron density profiles corresponding to the different sign combinations of a_n for the polymer IVc1 in the S_{C_2} phase.

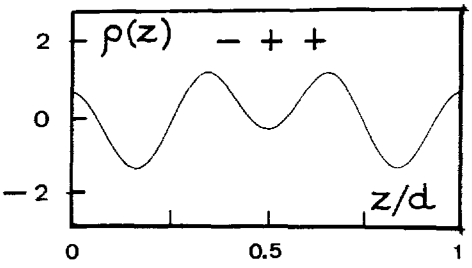

Figure 9. Projection of the electron density profile corresponding to the most physically acceptable sign combination ρ − + + for the S_{F_2} phase of the polymer IVc1.

I phase is known to be sharper than that of the F phase [13, 14]. The thickness of the wide angle reflection of our X-ray powder diagrams suggests that the smectic phase should be of the S_{F_2} type for the lower mesophase.

The occurrence of ordered (S_{F_2}) and disordered (S_{C_2}) phases is consistent with the observations by polarizing microscopy of the optical textures in the relevant temperature ranges; broken and striated fans in the S_{C_2} phase and more broken and truncated fans in the S_{F_2} phase.

4.3. *Polymers (IVb) R = CN*

These polymers exhibit as a function of temperature two disordered smectic mesophases (diffuse band in the wide angle domain of the X-ray patterns) differing in their layer thickness (see table 3). For the first one, d is smaller than $2l+p$, while for the second one it is slightly higher than $2l+p$.

In the low angle domain of the X-ray diagrams the second order of diffraction is absent, so there are only 4 possible electron density profiles for each smectic phase.

In the case of the lower smectic phase (see figure 10 (*a*)–(*d*)), for the same arguments as those used in the case of the polymers IVc, the four electron density profiles are incompatible with a partly interdigitated S_{A_d} smectic phase, and the profiles (*a*) and (*b*) are in agreement with a tilted, bilayer smectic S_{C_2}; however the electron density profile (*b*) corresponding to $\rho(z)$- + + is in better agreement with the electron densities of the different parts of the repeating unit of the polymer.

In the case of the upper phase, the double layer, perpendicular smectic S_{A_2} structure (d slightly higher than $2l+p$) is confirmed by the electron density profiles (see figure 11) and by the fibre X-ray diagram (see figure 12) showing a diffuse crescent on the meridian in the wide angle domain. We have verified that the fibre diagram corresponds to the upper mesophase by studying (with powder samples) the variation of the thickness d of the layers on cooling as a function of time. We have observed that the S_{A_2} phase transforms into the S_{C_2} phase only after some hours.

Therefore we can conclude that the upper mesophase is a double layer, perpendicular and disordered S_{A_2} phase, while the lower mesophase is a double layer, tilted and disordered S_{C_2} phase. These results are in agreement with the observations by polarizing microscopy: the upper mesophase is identified as smectic A by the appearance of characteristic focal-conic textures with fans, and on cooling, the fans became broken and striated fans in the S_{C_2} phase.

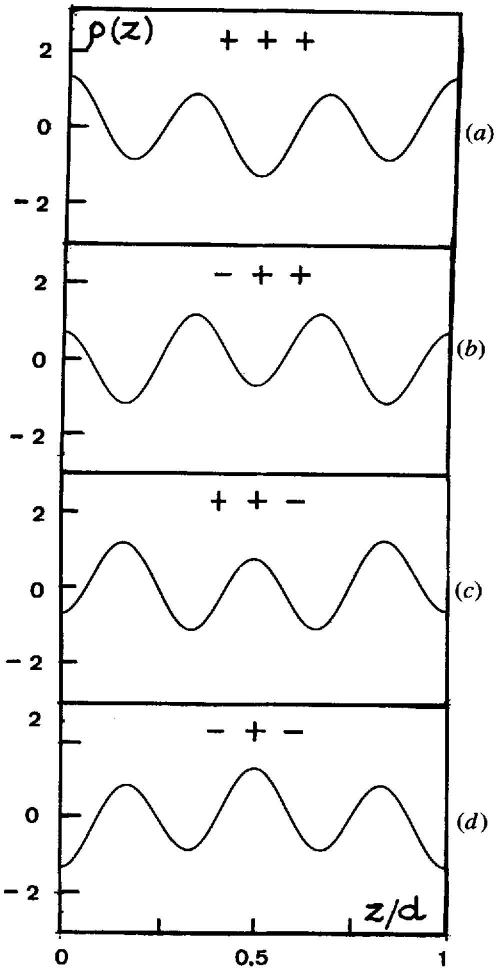

Figure 10. Projections of the electron density profiles corresponding to the different sign combinations of a_n for the polymer IVb1 in the S_{C_2} phase.

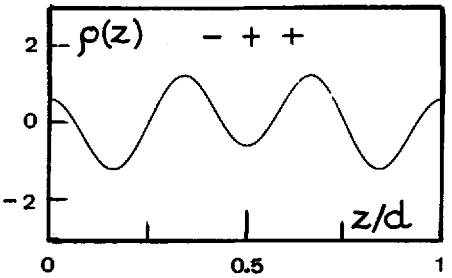

Figure 11. Projection of the electron density profile corresponding to the most physically acceptable sign combination ρ − + + for the S_{A_2} phase of the polymer IVb1.

4.4. *Polymers (IVa) R = H*

We showed recently [1] that such polymers exhibit, as a function of temperature, an ordered, tilted, bilayer smectic phase S_{I_2} and a disordered tilted bilayer smectic phase S_{C_2}.

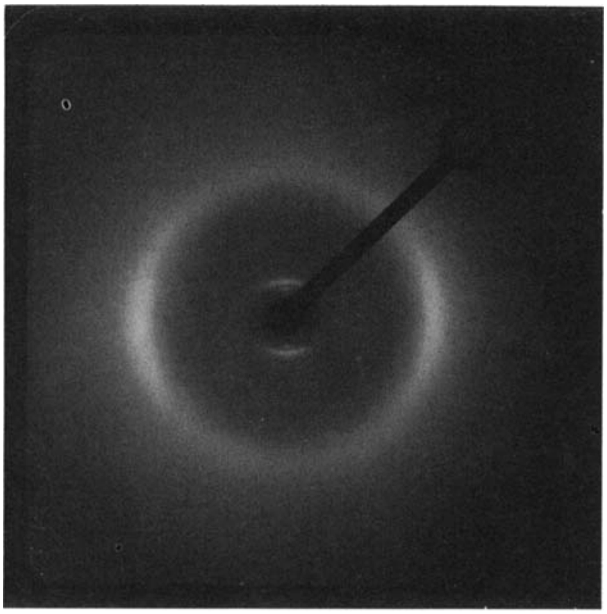

Figure 12. Pin-hole camera fibre X-ray diagram of the S_{A_2} mesophase of the polymer IVb1 at room temperature (vertical fibre axis); the first order small angle reflection is hidden by the beam-stop and the second order reflection is absent.

4.5. *Influence of temperature*

For the three families of polymers, within the whole temperature range of existence of one phase (S_{I_2}, S_{F_2}, S_{C_2} or S_{A_2}), the thickness *d* of the smectic layers is independent of temperature and remains constant (see figure 13). The values of the structural parameters found on heating were reversibly obtained on cooling, but for polymers IVb, the transformation S_{A_2}–S_{C_2} can take a few hours.

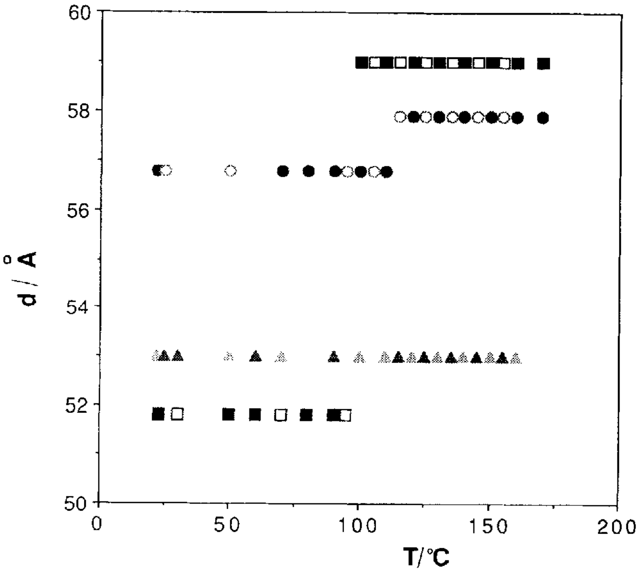

Figure 13. Variation with temperature (heating: full symbols and cooling: open symbols) of the layer thickness *d* of the smectic phases: polymer IVa triangles, polymer IVb squares, polymer IVc circles.

4.6. *Influence of the substituent R*

For the three types of polymers, two double layer smectic phases are observed as a function of temperature, but the nature of the phases and the values of the thickness *d* of the smectic layers are determined by the substituent *R* (see table 3). For $R = H$ the polymers exhibit successively S_{I_2} and S_{C_2} structures, for $R = CN$ S_{C_2} and S_{A_2} structures, and for $R = O\text{–}CH_2\text{–}CH(CH_3)\text{–}C_2H_5$ S_{F_2} and S_{C_2} structures.

Furthermore (see figure 13), there is no discontinuity in the layer thickness *d* at the transition S_{I_2}–S_{C_2} for $R = H$, a small increase of *d* at the transition S_{F_2}–S_{C_2} for $R = O\text{–}CH_2\text{–}CH(CH_3)\text{–}C_2H_5$, and large increase of *d* at the transition S_{C_2}–S_{A_2} for $R = CN$. But the geometric parameters (thickness *d* of the smectic layers) and the thermal domain of stability are the same for the chiral structures S_{F_2} and S_{C_2} of the polymer IVc1 as for the non-chiral structure S_{F_2} and S_{C_2} of the polymers IVc2 and IVc3.

4.7. *Influence of molecular weight*

For a fixed type of substituent *R*, the molecular weight of the polymer, at least in the range of molecular weights used in this study, has no influence on the types of mesophase, the values of their structural parameters and the transition temperatures.

5. Conclusions

In this paper, we have described the synthesis and the thermotropic behaviour of comb-like polymers with a polyacrylamide main chain, and a spacer of 10 methylene groups linked through an ester junction to a biphenyl, a cyanobiphenyl or a 2-methyl-1-butoxybiphenyl mesogenic group. All the three types of polyacylamide polymers are smectic at room temperature and exhibit as a function of temperature two different bilayer smectic phases, but the type of smectic phase is governed by the nature of the substituent *R* of the biphenyl core. For $R = H$, the polymers exhibit a double layer, ordered, tilted smectic S_{I_2} and a double layer, disordered, tilted smectic S_{C_2}. For $R = CN$, the polymers exhibit a double layer, disordered, tilted smectic S_{C_2} and a double layer, disordered, perpendicular smectic S_{A_2}. For $R = O\text{–}CH_2\text{–}CH(CH_3)\text{–}C_2H_5$, the polymers exhibit a double layer, ordered, tilted smectic S_{F_2} and a double layer, disordered, tilted smectic S_{C_2}, these two structures being chiral when the substituent *R* is chiral (polymer IVc1).

It is interesting to compare the behaviour of polyacrylamide polymers with polymers with different blackbones. A lot of work has been devoted to the study of the influence of the different fragments (blackbone, spacer, interconnecting group between the mesogen and the spacer, mesogen length and constitution) on the thermotropic behaviour of side-chain polymers ([15–17] and references therein). In particular, it has been shown that for fixed blackbone, spacer and mesogen, the nature of the connecting group between mesogen and spacer does not modify the type of mesophase [16]; therefore we can compare our polyacrylamide polymers with polymers with other main chains, even if they have different connecting groups between the mesogen and the spacer, on condition that the total number, m of carbon atoms of the spacer and the connecting group is the same.

In the case of polymers with cyanobiphenyl mesogenic groups and $m = 11$, polymers with polyacrylate main chains exhibit two interdigitated, disordered smectics S_{C_d} and S_{A_d} [18, 19], while polymers with polyacrylamide main chains exhibit two bilayer, disordered smectics S_{C_2} and S_{A_2}.

In the case of polymers with 2-methyl-1-butoxybiphenyl mesogenic groups and $m = 11$, polymers with polyacrylate main chains [20, 21] exhibit as a function of temperature a crystalline, a monolayer, metastable S_{C_1} and a monolayer smectic S_{A_1} phase, polymers with polysiloxane main chains exhibit a crystalline, a monolayer, ordered smectic S_{F_2}, and two monolayer, disordered smectics S_{C_1} and S_{A_1} [22], polymers with polyvinyl ether main chains exhibit a crystalline, a bilayer, disordered smectic S_{C_2} and a monolayer, disordered smectic S_{A_1} [23], while polymers with polyacrylamide main chains exhibit a bilayer, ordered smectic S_{F_2} and a bilayer, disordered smectic S_{C_2} phase.

Polymers with polyacrylamide main chains exhibit the highest smectogenic power as they give smectic mesophases at room temperature and the two smectic phases observed as a function of temperature are of the bilayer type.

On the contrary, the monomers of our acrylamide polymers do not exhibit liquid crystalline behaviour.

References

[1] Gallot, B., and Monnet, F., *Eur. Polym. J.* (in the press).

[2] Gallot, B., and Douy, A., 1987, *Molec. Crystals liq. Crystals*, **153,** 367.

[3] Gallot, B., and Marchin, B., 1989, *Liq. Crystals*, **5,** 1719.

[4] Gallot, B., and Diao, T., 1993, *Liq. Crystals*, **14,** 947.

[5] Gallot, B., and Marchin, B., 1989, *Liq. Crystals*, **5,** 1729.

[6] Kabalka, G. W., Varma, M., and Varma, R. S., 1986, *J. org. Chem.*, **51,** 2386.

[7] Zentel, R., Reckert, G., and Reck, B., 1987, *Liq. Crystals*, **2,** 83.

[8] Davidson, P., Levelut, A. M., Achard, M. F., and Hardouin, F., 1989, *Liq. Crystals*, **4,** 561.

[9] Neises, B., and Stieglish, W., 1978, *Angew. Chem. Int. Ed. Engl.*, **17,** 522.

[10] Hofle, G., Stieglish, W., and Vorbruggen, H., 1978, *Angew. Chem. Int. Ed. Engl.*, **17,** 569.

[11] De Vries, A., 1985, *Molec. Crystals liq. Crystals*, **131,** 125.

[12] Gudkov, V. A., 1984, *Soviet Phys. Crystallogr.*, **29,** 316.

[13] Benattar, J. J., Moussa, F., and Lambert, M., 1981, *J. Phys. Lett.*, **42,** 167.

[14] Benattar, J. J., Moussa, F., and Lambert, M., 1983, *J. chem. Phys., chem. Biol.*, **80,** 99.

[15] Shibaev, V. P., and Plate, N. A., 1985, *Pure appl. Chem.*, **57,** 1589.

[16] Percec, C., and Pugh, C., 1989, *Side-chain Liquid Crystal Polymers*, edited by C. B. McArdle (Blackie and Sons, Glasgow), Chap. 3.

[17] Imrie, C. T., Karasz, F. E., and Attard, G. S., 1993, *Macromolecules*, **26,** 3803.

[18] Shibaev, V. P., Kostromin, S. G., and Plate, N. A., 1982, *Eur. Polym. J.*, **8,** 651.

[19] Kostromin, G. S., Sinitzyn, V. V., Talroze, R. V., and Shibaev, V. P., 1982, *Makromolek. Chem. rap. Commun.*, **3,** 809.

[20] Ringsdorf, H., Urban, C., Knoll, W., and Sawodny, M., 1992, *Makromolek. Chem.*, **193,** 1235.

[21] Chiellini, E., Galli, G., Cioni, F., Dossi, E., and Gallot, B., 1993, *J. mater. Chem.*, **3,** 165.

[22] Gailot, B., Galli, G., Dossi, E., and Chiellini, E., 1995, *Liq. Crystals*, **18,** 463.

[23] Chiellini, E., Dossi, E., Galli, G., Solaro, R., and Gallot, B., *Macromolek. Chim. Phys.* (submitted).